Four-dimensional Flow MRI: Principles and Cardiovascular Applications

Arshid Azarine, MD, MSc
Philippe Garçon, MD
Audrey Stansal, MD
Nadia Canepa, MD
Giorgios Angelopoulos, MD
Stephane Silvera, MD
Daniel Sidi, MD
Véronique Marteau, MD
Marc Zins, MD

Abbreviations: CHD = congenital heart disease, 4D = four-dimensional, IVC = inferior vena cava, PC = phase-contrast, SVC = superior vena cava, 3D = three-dimensional, 2D = two-dimensional, WSS = wall shear stress

RadioGraphics 2019; 39:632–648

https://doi.org/10.1148/rg.2019180091

Content Codes: CA CH MR VA

From the Departments of Medical Imaging (A.A., N.C., G.A., S.S., V.M., M.Z.), Cardiology (P.G.), and Vascular Medicine (A.S.), Saint Joseph Hospital, 185 rue Raymond Losserand, 75014 Paris, France; and Department of Pediatric Cardiology, Necker Enfants Malades Hospital, Paris, France (D.S.). Presented as an education exhibit at the 2017 RSNA Annual Meeting. Received March 15, 2018; revision requested May 23 and received July 9; accepted July 24. For this journal-based SA-CME activity, the author A.A. has provided disclosures (see end of article); all other authors, the editor, and the reviewers have disclosed no relevant relationships. **Address correspondence to** A.A. (e-mail: *aazarine@hpsj.fr*).

See discussion on this article by Ordovas (pp 648–650).

In-plane phase-contrast (PC) imaging is now a routine component of MRI of regional blood flow in the heart and great vessels. Inplane PC MRI provides a volumetric, isotropic, time-resolved cine sequence that enables three-directional velocity encoding, a technique known as four-dimensional (4D) flow MRI. Recent advances in 4D flow MRI have shortened imaging times, while progress in big-data processing has improved dataset pre- and postprocessing, thereby increasing the feasibility of 4D flow MRI in clinical practice. Important technical issues include selection of the optimal velocity-encoding sensitivity before acquisition and preprocessing of the raw data for phase-offset corrections. Four-dimensional flow MRI provides unprecedented capabilities for comprehensive analysis of complex blood flow patterns using new visualization tools such as streamlines and velocity vectors. Retrospective multiplanar navigation enables flexible retrospective flow quantification through any plane across the volume with good accuracy. Current flow parameters include forward flow, reverse flow, regurgitation fraction, and peak velocity. Four-dimensional flow MRI also supplies advanced flow parameters of use for research, such as wall shear stress. The vigorous burgeoning of new applications indicates that 4D flow MRI is becoming an important imaging modality for cardiovascular disorders. This article reviews the main technical issues of 4D flow MRI and the different parameters provided by it and describes the main applications in cardiovascular diseases, including congenital heart disease, cardiac valvular disease, aortic disease, and pulmonary hypertension.

Online supplemental material is available for this article.

SA-CME LEARNING OBJECTIVES

After completing this journal-based SA-CME activity, participants will be able to:

- Explain the technical principles of 4D flow MRI.
- Describe the current and advanced tools provided by 4D flow MRI in cardiovascular disease.
- Discuss the established and potential indications of 4D flow MRI in cardiovascular disease.

See rsna.org/learning-center-rg.

Introduction

Standard two-dimensional (2D) phase-contrast (PC) MRI was introduced in the late 1980s to enable through-plane assessment of blood flow fields and velocities, particularly in the cardiovascular system (1–3). Since then, the development of in-plane PC sequences has allowed acquisition of a time-resolved cine sequence amenable to three-dimensional (3D) velocity encoding, a technique known as four-dimensional (4D) (3D plus time) flow MRI. Although 4D flow MRI was introduced in the 1990s (4), it entered the field of clinical practice only recently, after multiple improvements produced faster sequences, lighter datasets, big-data analysis software that was more user-friendly and accurate, more powerful graphics processing units (GPUs), and cloud-based postprocessing. In addition to providing the basic PC findings such as peak velocity, flow volume, and flow direction, 4D flow MRI delivers unprecedented capabilities for comprehensive blood flow assessment, offering various modalities of blood flow pathway visualization and thereby helping one understand blood flow changes and retrospectively perform accurate flow measurements (5,6).

TEACHING POINTS

- The development of in-plane PC sequences has resulted in acquisition of a volumetric time-resolved cine sequence enabling 3D velocity encoding, a technique known as 4D (3D plus time) flow MRI.
- Four-dimensional flow MRI provides unprecedented capabilities for comprehensive blood flow assessment via blood flow visualization using color-coded 3D multiplanar reformations, streamlines, and velocity vectors.
- Four-dimensional flow MRI allows retrospective navigation, thereby providing optimal measurement of any blood flow at any level of a given vessel within the acquired volume.
- Four-dimensional flow MRI provides new advanced parameters for use in research, such as wall shear stress (WSS), kinetic energy loss, and pressure difference fields.
- Although cardiac 4D flow MRI is chiefly used and studied in CHD, the spectrum of indications is expanding rapidly to other fields such as cardiac valvular disease, aortic aneurysm and stenosis, pulmonary hypertension, portal hypertension, and cerebral artery aneurysm.

In this article, we review the main technical issues of 4D flow MRI and the parameters provided by it and describe the main applications in cardiovascular diseases, including congenital heart disease (CHD), cardiac valvular disease, aortic disease, and pulmonary hypertension.

From 2D to 4D Flow Imaging

The development of in-plane PC sequences has resulted in acquisition of a volumetric time-resolved cine sequence enabling 3D velocity encoding, a technique known as 4D (3D plus time) flow MRI.

Two-dimensional PC MR images are acquired with single-direction (through-plane) velocity encoding during a breath hold. When flow must be measured at several sites, the acquisition must be repeated at each site, taking care to position the acquisition plane perpendicular to the long axis of the vessel of interest, a technically challenging and time-consuming process that may also be difficult for patients, particularly those with complex CHD. Whereas the standard 2D PC sequence provides an image with a single velocity and magnitude, 4D flow MRI provides sets of 3D volumes over time (4D). Each 4D volume contains one magnitude volume and three velocity volumes encoded in the three dimensions of space (Fig 1).

Technical Considerations

Before starting 4D flow MRI acquisition, several technical points must be considered to ensure that signal-to-noise ratio and velocity-to-noise ratio are optimal and to produce sufficient spatial and temporal resolution. However, the parameters should be adapted and optimized for each case. A technical checklist can be useful (Table).

Preparation

The patient should be informed that the acquisition time for 4D flow MRI is relatively long. To reduce artifacts and ensure optimal and homogeneous data acquisition, patients should be instructed to breathe naturally and regularly for 7–10 minutes, depending on the data acquisition time. In most cases, patients should also be prepared for an intravenous injection of gadolinium-based contrast agent via a power injector.

Electrocardiographic Gating

For all anatomic regions, 4D flow MRI is synchronized to the heartbeat. Synchronization must cover the entire cardiac cycle with consistency across R-R intervals (7). Thus, reliable retrospective electrocardiographic (ECG) gating is crucial for 4D flow MRI. Using retrospective rather than prospective gating enables full coverage of the cardiac cycle. New self-gating techniques are being evaluated by some manufacturers (8).

Respiratory Gating

Because respiratory motion may affect 4D flow MRI data, thoracic and abdominal images are typically acquired using adaptive diaphragm navigator gating. When a fixed acceptance gating window is used, acquisition efficiency can vary widely. Owing to interindividual variability in breathing patterns, total acquisition time can range from 6 to 15 minutes, depending on acquired volume or spatial resolution.

Many authors have described free-breathing 4D flow MRI (8) without respiratory gating, which results in shorter acquisition times. Several motion-suppression techniques are effective in minimizing errors associated with respiratory motion. Whether respiratory gating should be used for 4D flow MRI remains debated (9).

Pulse Sequence

Four-dimensional flow MRI is based on short echo time (TE) and repetition time (TR) radiofrequency-spoiled gradient-echo sequences (TR = 5–7 msec, TE = 2–4 msec).

Contrast Medium

Four-dimensional flow MRI can be performed without contrast agent. Use of contrast agent significantly improves signal-to-noise ratio in magnitude data and noise reduction in velocity data compared to measurements without contrast agent (10). The concentration and relaxivity of the contrast agent, the acquisition technique, and the injection protocol may influence image quality (11).

We recommend using a macromolecular contrast agent for safety reasons. Several injection

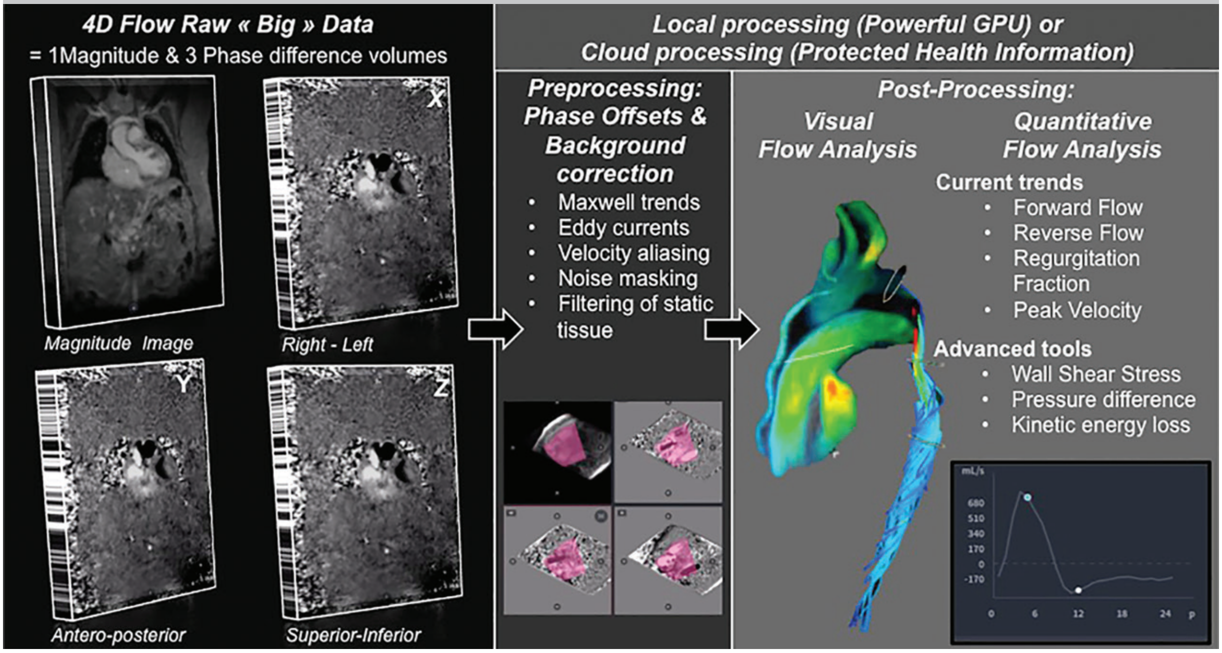

Figure 1. Four-dimensional flow MRI provides sets of 3D volumes over time (4D). Each 4D volume contains one magnitude volume and three phase-difference volumes encoded in the three directions of space (x, y, z). Raw data are preprocessed then postprocessed using local or online software. After preprocessing for phase-offset correction, retrospective postprocessing starts with visual analysis followed by quantitative analysis of the datasets. *GPU* = graphics processing unit.

protocols are available. We use a triphasic protocol, starting with a bolus of contrast agent (flow rate, 3–4 mL/sec) followed by a slow infusion (0.1–0.2 mL/sec) and finally by a small saline flush injection.

Acquisition Time
For thoracic 4D flow MRI, the acquisition time is 5–8 minutes without respiratory gating and up to 10–15 minutes with respiratory gating.

Velocity Encoding Sensitivity
As with 2D PC sequences, blood velocities exceeding the velocity encoding (VENC) result in velocity aliasing, precluding flow measurements. Hence, VENC is usually set at 10% above the expected maximum velocity (7). However, high VENC increases noise and decreases velocity-to-noise ratio, especially in regions of low velocity; therefore, the best compromise should be sought.

If velocity aliasing occurs, phase unwrapping algorithms may help, although the available applications use different strategies and do not always allow optimal measurements. Different investigators and manufacturers advocate new multi- or dual-VENC strategies during acquisition to reliably incorporate both low- and high-velocity fields with optimal velocity-to-noise ratio (12).

Temporal Resolution
Temporal resolution is ideally set below 40 msec. To reduce the acquisition time, decreasing temporal resolution up to 60 msec has been advocated in specific situations, despite the negative effect on flow quantification and visualization accuracy (7).

Spatial Resolution
The setting for spatial resolution depends on the region of interest and field of view. Ideally, isotropic spatial resolution of about 1.5–3.0 mm^3 is recommended for the great vessels and thoracoabdominal area in adults (7) (Table). Coronal or sagittal acquisitions provide more extensive coverage. Axial acquisition is suitable for smaller coverage (less risk of wrapping artifact).

Pre- and Postprocessing of Raw Data
Four-dimensional flow MRI generates a huge number of datasets, from which a wide variety of flow-specific images and information can be derived. Retrospective navigation allows highly accurate analysis of the datasets at any moment after acquisition (Fig 1).

Big-Data Management

Local Software.—Various types of software are available for direct local transfer and processing of big data. The advantage of this approach is that pre- and postprocessing are performed locally. The main issues are the time-consuming nature of the processing and the need for powerful computers with high-performance GPUs (graphics processing units) and considerable random-access memory.

Technical Checklist for 4D Flow MRI

Parameter	Recommendations	Reasons	Comments
ECG gating	Retrospective	Avoid sequence interruption Cover entire R-R cycle	Crucial for all anatomic areas
VENC	Maximum velocity expected (10% higher when possible)	Avoid velocity aliasing	The higher the VENC, the lower the VNR Use multiple VENCs if available
Temporal resolution	Optimal <40 msec Avoid >60 msec About 20–50 cardiac frames	Accuracy	Arterial/cardiac studies ≥20 cardiac frames Venous studies ≥14 cardiac frames
Spatial resolution	Maximum, isotropic voxels, 2.0–2.5 mm^3 for aorta and pulmonary artery	Accuracy	About five voxels in vessel of interest
Field of view	Maximum	Better SNR and coverage	Cover region of interest
Flip angle	A bit higher than Ernst angle	Better CNR	Higher if use of contrast agent
Contrast agent	Macromolecular	Larger coverage Better SNR	Bolus followed by very slow perfusion
Offset errors correction	Eddy current correction, phase unwrapping…	Accuracy Correction of offsets	Check eddy current correction before flow measurement

Note.—CNR = contrast-to-noise ratio, ECG = electrocardiography, SNR = signal-to-noise ratio, VENC = velocity encoding, VNR = velocity-to-noise ratio.

Online Software.—The dataset is uploaded to a dedicated Web-based software application (ie, Arterys; San Francisco, Calif), considering local regulations for protection of personal health information (PHI). A secure PHI system must be used. As dataset size ranges from 2 to 4 gigaoctets, a good Internet connection is crucial. Once the dataset is uploaded, the software ensures rapid online pre- and postprocessing and fluent retrospective analysis. This method improves workflow and can be used from any device anywhere in the world.

Dataset Preprocessing

As with 2D cine PC imaging, various changes in gradient fields result in varying spatial and temporal phase offsets. Data preprocessing should include intrinsic automatic or semiautomatic phase-offset corrections for Maxwell terms, eddy currents, and phase wraps resulting in velocity aliasing (7). Optimal corrections for background phase offsets may vary across MRI systems and postprocessing applications (Fig 1).

Dataset Postprocessing and Analysis

Four-dimensional flow MRI provides unprecedented capabilities for comprehensive blood flow assessment via blood flow visualization using color-coded 3D multiplanar reformations, streamlines, and velocity vectors.

Visual Analysis

Multiple options provide new capabilities for a comprehensive and interactive approach to flow analysis via application of various visualization modalities to the volumetric, time-resolved, velocity-encoded dataset (Fig 2).

3D PC MR Angiography

Three-dimensional PC MR angiography provides anatomic orientation for flow visualization and regional flow quantification. Three-dimensional maximal intensity projection (MIP), isosurface rendering, or other options can be used.

Color Coding

As with echo Doppler US, adding color coding with an adjustable scale to 3D PC MR angiography enables visualization of low and high velocities within the volume at a glance. In general, red is used for high velocities and blue for low velocities.

Streamlines

Streamlines show the path a particle would take if released into the velocity field, with the field held constant (Fig 2b) (Movie 1). Streamlines were introduced for nongated carotid artery imaging in the 1990s (2) and were subsequently improved and time resolved by Buonocore (13). Streamlines allow characterization of the blood flow pattern as follows:

Laminar Flow.—Normal flow is laminar and central (Fig 2b).

Helical Flow.—The particles rotate around an axis of flow while also exhibiting net forward motion

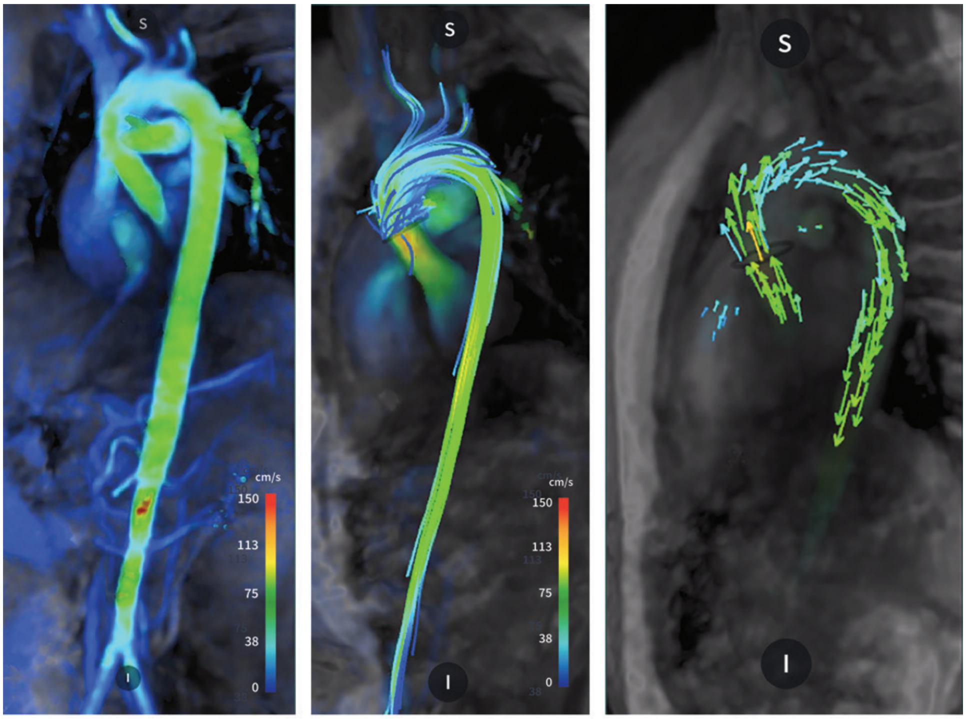

a. b. c.

Figure 2. Different modalities for visual analysis of aortic blood flow in a 24-year-old woman with a mild form of abdominal Takayasu arteritis. **(a)** Color-coded 3D rendering shows areas of high velocity (red). The color scale is adjustable according to the vessel of interest. **(b)** Color-coded 3D rendering with streamlines shows a normal laminar blood flow pattern. Streamlines show the path a particle would take if released into the velocity field, with the field held constant. **(c)** Color-coded 3D rendering shows velocity vectors, which display the velocity and direction of blood flow. In all figures, orientations are labeled as follows: *A* = anterior, *I* = inferior, *L* = left, *P* = posterior, *R* = right, *S* = superior.

parallel to the axis, producing helical streamlines (Fig 3a). Initial jet flow may be eccentric, with high-velocity flows near the vessel wall (Fig 3b).

Vortical Flow.—Rotating or swirling motion occurs in the flow field, with streamlines or path lines tending to curl back on themselves, as in a whirlpool. Hence, the streamlines are concentric circles (Fig 3c).

Velocity Vectors

Velocity vectors indicate the speed and direction of blood velocity (Fig 2c). An arrow can be used to represent both the magnitude and the direction of velocity at a given point, calculated from the magnitudes of the x, y, and z components of velocity.

Conventional Quantitative Analysis

Four-dimensional flow MRI allows retrospective navigation, thereby providing optimal measurement of any blood flow at any level of a given vessel within the acquired volume.

When performing quantitative analysis of 4D flow MRI data, several methodological issues must be considered.

Eddy currents may result in background phase errors that can seriously affect flow measurements. An appropriate strategy for correction of phase offset errors due to eddy currents should be applied before further processing. Using a stationary fluid-filled phantom is a complex and less used strategy to establish a baseline of zero velocity. The most commonly used approach is manual thresholding to identify static tissues, eventually associated with identification of different anatomic structures within the acquisition, or manually limiting the field of interest. Some postprocessing software programs propose already advanced algorithms enabling semiautomatic thresholding.

Vendors and postprocessing software programs are working on deep learning–based approaches already used for cardiac segmentation to improve the accuracy and speed of this correction process. However, quality control is essential for each 4D flow MRI study. Applying the conservation-of-mass principle is an excellent option for checking the reliability of flow volume quantification for each study, particularly when imaging the heart and great vessels. This option may be used as the first in-line quality control step (7). Furthermore, given its volumetric coverage, 4D flow MRI offers several opportunities for controlling internal data

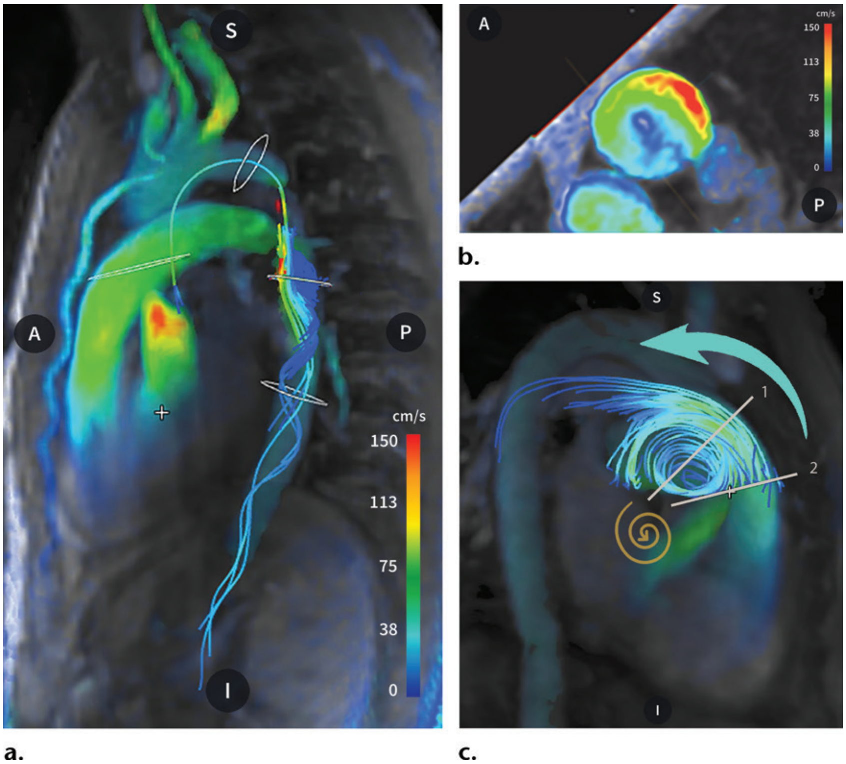

Figure 3. Four-dimensional flow MRI provides a comprehensive view of different blood flow patterns. **(a)** Image with streamlines in a young adult with severe aortic coarctation shows aortic poststenotic helical flow in the descending aorta during systole. **(b)** Cross-sectional view of the ascending aorta in a patient with a bicuspid aortic valve shows eccentric high-velocity jet flow (red) adjacent to the lateral aortic wall. **(c)** Image with streamlines shows systolic pulmonary artery forward flow (blue arrow) in a young adult with pulmonary regurgitation 18 years after tetralogy of Fallot repair. The streamlines also demonstrate vortical flow (gold arrow) in the aneurysmal pulmonary artery. Streamline visualization improves positioning accuracy for blood flow measurement perpendicular to the axis of the vessel (levels 1 and 2) and allows avoidance of areas of vortical flow (level 2), thus improving the accuracy of assessment of pulmonary regurgitation severity. Pulmonary regurgitation was estimated to be severe (level 1) or moderate (level 2).

consistency. Use of routine phantom calibration to subtract potential background phase offsets when possible has been recommended (7).

Flow Measurement

Use of 3D or 4D PC MR angiography derived from 4D flow MRI data helps with anatomic orientation and identification of cross-sectional analysis planes for flow quantification. Retrospective navigation enables highly accurate positioning for blood flow measurement, usually perpendicular to the axis of the vessel. Streamline visualization improves positioning accuracy for flow measurements by avoiding areas with turbulent flow patterns such as vortical flows (Fig 3c). Flow measurements can be retrospectively calculated in regions not previously suspected to be relevant, and this is probably one of the most important advantages of 4D flow MRI compared with multiple 2D velocity sequences performed at different specific locations. New measurement sites can be assessed retrospectively and interactively, and new strategies can be developed to refine the diagnosis (6).

Once the boundaries of a given vessel are drawn, automatic segmentation is usually performed by the software for all cardiac time frames. This segmentation process can be expected to benefit from machine learning or deep learning. As always, automatically detected flow contours must be checked over the entire cardiac cycle to avoid measurement errors due to the involvement—for some phases—of other flows within the boundaries. This type of error is particularly likely to occur at the heart and great vessels. Forward flow, reverse flow (in milliliters per beat), regurgitation fraction (in percent), and peak velocity (in meters per second) are parameters currently provided by flow measurement (Fig 1).

Advanced Features for Research

Four-dimensional flow MRI provides new advanced parameters for use in research, such as wall

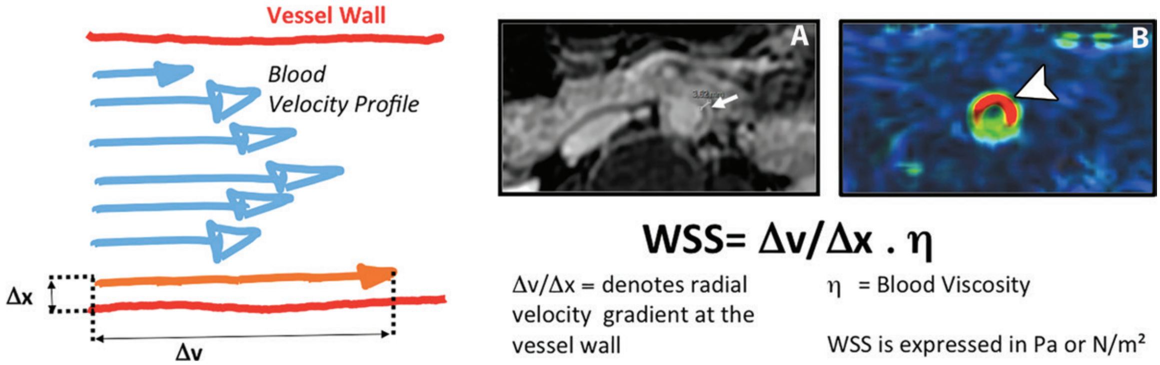

Figure 4. Four-dimensional flow MRI–derived WSS estimates viscous shear forces from blood flow directed tangential to the vessel wall. Eccentric high-velocity flow (orange arrow) adjacent to the aortic wall increases regional WSS and may induce aortic wall remodeling. *A,* Postcontrast T1-weighted MR image in a young patient with active Takayasu disease shows thickening of the abdominal aortic wall to 3.5 mm (arrow). *B,* WSS color map at the same level shows increased regional WSS (red) at the anterior aortic wall (arrowhead).

shear stress (WSS), kinetic energy loss, and pressure difference fields.

Wall Shear Stress

WSS refers to the stress applied tangentially to the vessel wall, that is, the tangential viscous shear forces per unit area exerted by shear in the fluid layer immediately adjacent to the wall (fluid-wall shear stress). WSS reflects the effect of flow changes on endothelial-cell and extracellular-matrix function (14,15). Four-dimensional flow MRI–derived WSS helps determine the site of greatest shear stress on the vessel wall (Fig 4). A 2D or 3D WSS map may help identify areas at risk for rupture in aneurysms (16).

Pulse-Wave Velocity

Pulse-wave velocity is the velocity of pulse-wave propagation along a vessel, usually an artery. Pulse-wave velocity is normally several times faster than the blood flow velocities within the vessel (17).

Turbulence Kinetic Energy, Viscous Energy Loss, Pressure Difference Fields

These parameters have been described as new tools for research (17), although pitfalls in their determination persist and the best measurement strategies remain unclear (18). Pressure difference maps derived from 4D flow MRI may depict alterations in spatial pressure distribution (19), although further validation of this possibility is needed.

Clinical Applications

Although cardiac 4D flow MRI is chiefly used and studied in CHD, the spectrum of indications is expanding rapidly to other fields such as cardiac valvular disease, aortic aneurysm and stenosis, pulmonary hypertension, portal hypertension, and cerebral artery aneurysm.

In the following sections, we review the main indications for 4D flow MRI. This technique was readily adopted for evaluation of aortic abnormalities and CHD. However, the spectrum of 4D flow MRI indications is expanding steadily. For indications not discussed herein, readers are referred to the literature.

Congenital Heart Disease

Although transthoracic echocardiography is the first-line cardiovascular imaging modality for adults with CHD, 4D flow MRI is increasingly used as a means of obtaining accurate values for difficult flow measurements (eg, pulmonary regurgitation). Cardiac MRI is the current reference standard for measuring both right and left ventricular volumes (20,21). The more complex the CHD, the greater the usefulness of cardiac 4D flow MRI in understanding the disease and providing guidance for planning surgery or other treatments. In addition to diagnosis and comprehensive evaluation of CHD in infants and adults, areas that are benefiting from cardiac 4D flow MRI include follow-up of patients with complex surgically treated grown-up CHD.

Shunts and Anomalous Pulmonary Venous Return.—Echocardiography is the modality of choice for visualizing atrial septal defect (ASD), ventricular septal defect, and patent ductus arteriosus (PDA). Cardiac MRI allows clarification of the amount of shunting, assessment of biventricular size and function, and most important, detection of associated anomalies such as anomalous pulmonary venous return (APVR). These data are crucial for planning interventions (22,23). The volumetric coverage of cardiac 4D flow MRI improves visualization of sinus venosus, APVR, and other shunts that are difficult to assess with transthoracic echocardiography (Movie 2).

Figure 5. Incidental shunts diagnosed using cardiac 4D flow MRI. **(a)** Magnitude image shows major right ventricular dilatation in a teenage athlete referred for palpitations and right ventricular dilatation at transthoracic echocardiography without detectable shunting. The good global and regional right ventricular function ruled out right ventricular cardiomyopathy. *LV* = left ventricle, *RV* = right ventricle. **(b)** Image with streamlines shows a left-to-right shunt through an inferior ASD. **(c)** Image with velocity vectors shows a left-to-right shunt. **(d)** Superior left APVR (arrowhead) is also seen. **(e, f)** Subsequently, flow was assessed using multiplanar navigation to optimally measure Q_P/Q_S, which was significant ($Q_P/Q_S = 3$). This finding combined with the major right ventricular dilatation suggested that intervention was in order. Also note the pulmonary artery dilatation and high-velocity blood flow in the pulmonary arteries. *1* = contour of ascending aorta, *2* = contour of pulmonary artery. **(g)** Image with velocity vectors shows right-to-left shunting, consistent with severe pulmonary hypertension in a sinus venosus ASD with inferior right APVR, which was found incidentally in a symptomatic 70-year-old man. *LA* = left atrium, *LV* = left ventricle, *RA* = right atrium, *RVOT* = right ventricular outflow tract.

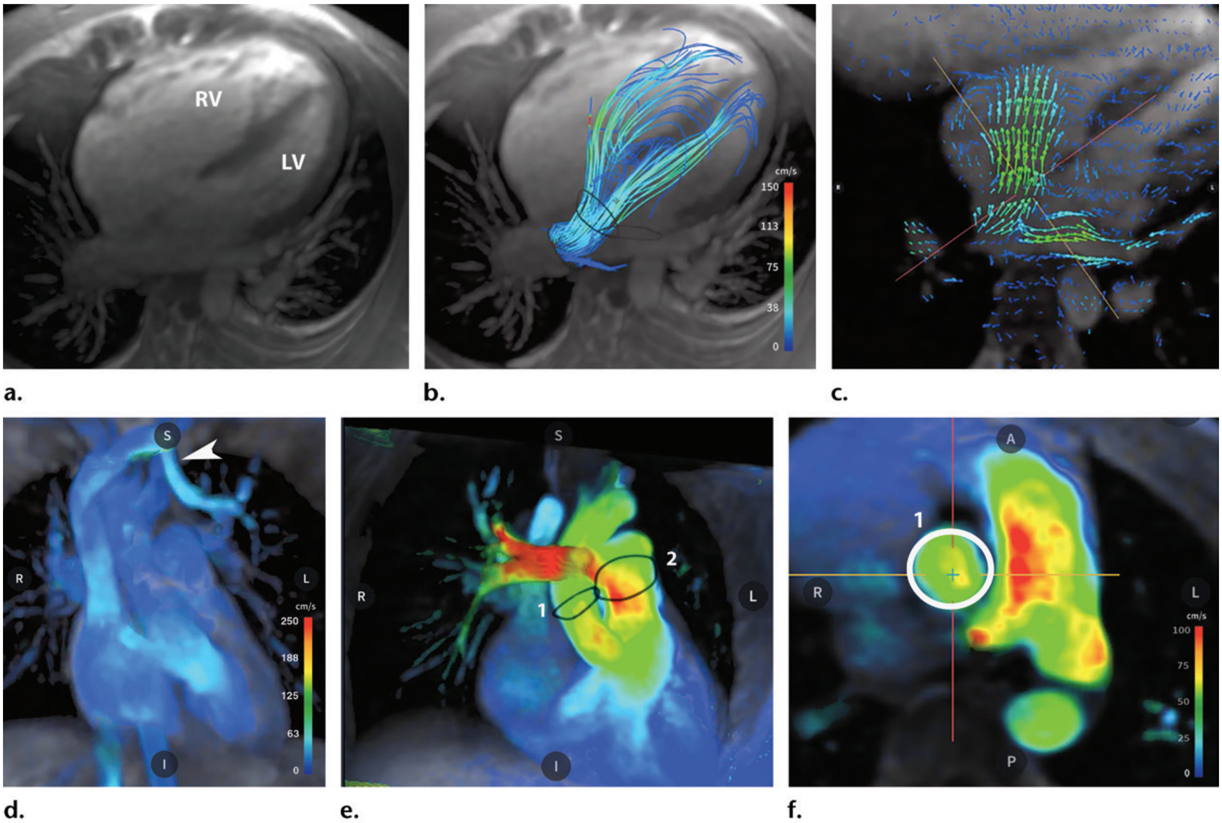

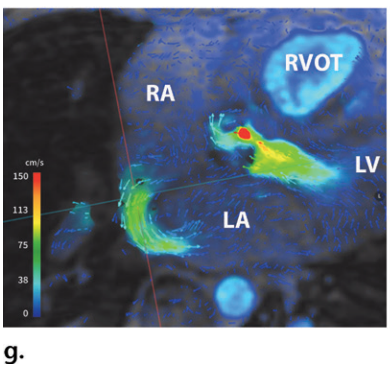

Systemic flow (Qs) in the ascending aorta and pulmonary flow (Qp) in the pulmonary artery can be estimated retrospectively to evaluate intracardiac left-to-right shunting (significant if Qp/Qs > 1.5). If PDA, septal defect, APVR, or other abnormalities are detected subsequently, flow measurements can be reliably assessed retrospectively in optimally positioned planes (Fig 5). Interestingly, in advanced ASD, temporary or permanent shunt inversion (right to left) due to pulmonary hypertension can be demonstrated by analyzing the velocity vectors (Fig 5g).

Follow-up of Patients with Fontan Circulation.—Fontan operations are performed in children with a single effective ventricle (severe hypoplastic left or right heart syndrome). The systemic and pulmonary vascular beds are surgically connected in series downstream of the single effective ventricle. This cavopulmonary connection eliminates shunting at the cost of a major increase in systemic venous pressure, which maintains flow through the lungs (24).

Cardiac 4D flow MRI has been used to assess flow shunting in post–Fontan operation patients (25). Streamlines help illustrate the spatial distribution and dynamics of blood flow from the inferior vena cava (IVC) or superior vena cava (SVC) to each pulmonary artery (Movie 3). Nonuniform mixing of blood to the left and right pulmonary arteries has been reported, with substantial interindividual differences despite similar

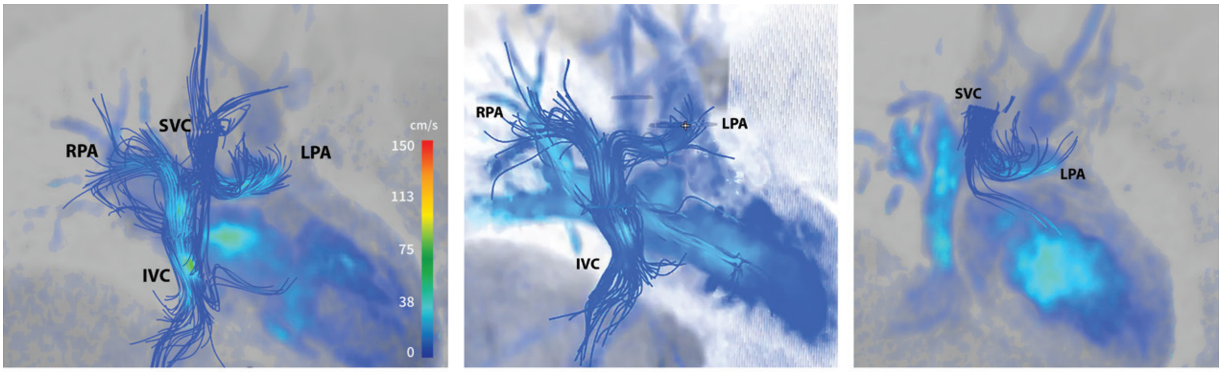

a. b. c.

Figure 6. Single ventricle and Fontan circulation in a young patient. *LPA* = left pulmonary artery, *RPA* = right pulmonary artery. **(a)** Image with streamlines shows patent cavopulmonary connections with relatively uniform distribution of venous return from the SVC and IVC. **(b)** Image of streamlines from the IVC shows uneven distribution of hepatic-rich venous return from the IVC connection predominantly directed toward the right lung. **(c)** Image of streamlines from the SVC shows that flow is predominantly directed toward the left pulmonary artery.

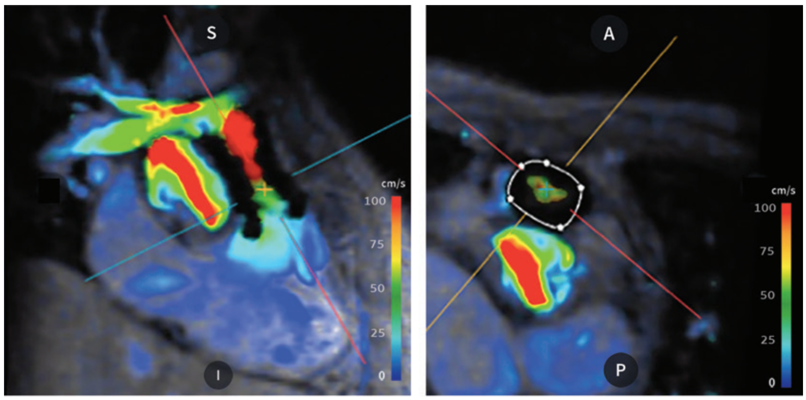

a. b.

Figure 7. Free-breathing 4D flow MRI enabling accurate follow-up of repaired tetralogy of Fallot in a 19-year-old man with CHARGE syndrome who also underwent transcatheter pulmonary valve implantation for severe pulmonary regurgitation. **(a)** Color-coded 3D maximum intensity projection image shows increased velocity (red) in the implanted pulmonary valve and right pulmonary artery, suggestive of mild stenosis. No significant susceptibility artifact is visible. **(b)** Cross-sectional view of the pulmonary artery enabling flow measurements shows no residual pulmonary regurgitation.

Fontan geometry (Fig 6). This uneven distribution of hepatic-rich venous return from the lower body to the left and right lungs (via the IVC) may influence development of serious complications such as pulmonary arteriovenous malformations and fistulas (25).

Valverde et al (25) found good agreement between flow shunting measurements with cardiac 4D flow MRI and 2D PC MRI in patients with systemic-to-pulmonary collateral flow. In addition, cardiac 4D flow MRI allows quantification of intra- and extraventricular kinetic energy and comparison of energy loss in patients with Fontan circulation, which may be relevant for planning surgery or an interventional procedure (26).

Repaired Tetralogy of Fallot.—Major issues in many patients with repaired tetralogy of Fallot include evaluation of free or almost free pulmonary regurgitation, pulmonary artery patency, and right ventricular size and function. Cardiac MRI with 2D PC sequences provides most of the information needed during follow-up of patients after tetralogy of Fallot repair.

In this population, cardiac 4D flow MRI has documented variations in flow characteristics (27). Flow vortex formation in the pulmonary trunk and pulmonary arteries, as well as higher right/left pulmonary artery blood flow ratios, were observed (27). Vortical flows in an aneurysmal pulmonary artery may induce offsets in pulmonary regurgitation evaluation. Streamline visualization improves the accuracy of positioning for blood flow measurement by avoiding areas of vortical flow (Fig 3c).

Tetralogy of Fallot can occur in patients with Down syndrome or CHARGE syndrome, in whom the repeated breath-holds needed for cardiac MRI are difficult to achieve. Free-breathing cardiac 4D flow MRI overcomes this difficulty and improves measurement accuracy. After transcatheter pulmonary valve repair for pulmonary regurgitation, cardiac 4D flow MRI provides optimal flow measurements with minimal susceptibility artifacts (Fig 7).

Follow-up after Senning Atrial Switch Surgery.—Specialist knowledge is needed to assess grown-up patients with CHD who have undergone the

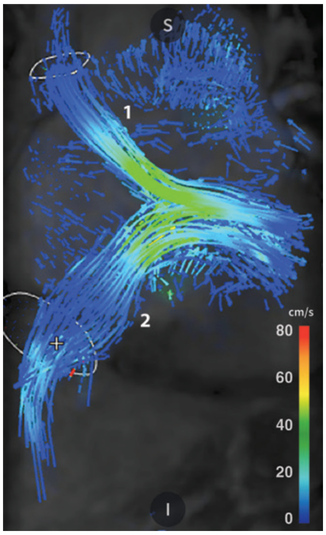

Figure 8. Four-dimensional flow MRI in a 22-year-old woman with Senning circulation. Image with streamlines shows patency of the reimplanted SVC and IVC and absence of stenosis along their course to the mitral valve. *1* = streamlines from SVC, *2* = streamlines from IVC.

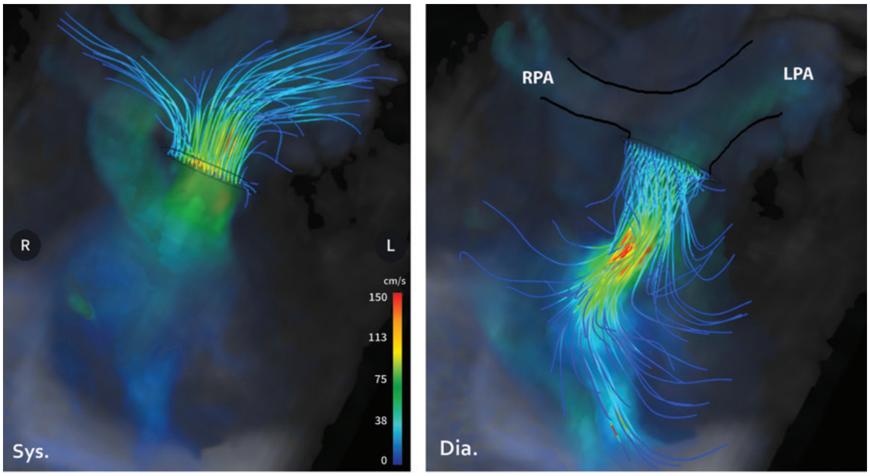

a. **b.**

Figure 9. Isolated pulmonary regurgitation in a 40-year-old man. **(a)** Image with streamlines during systole *(Sys)* shows laminar flow without regional vortices. **(b)** Image with streamlines during diastole *(Dia)* shows reverse flow. Pulmonary regurgitation was moderate with a regurgitation fraction of 35%. *LPA* = left pulmonary artery, *RPA* = right pulmonary artery.

Mustard or Senning operation for transposition of the great arteries. In the past decade, correction by atrial switch has gained popularity, as it makes the left ventricle the systemic ventricle. Nevertheless, many grown-up patients with CHD are still referred for follow-up after atrial switch surgery (24). Patency or stenosis of the reimplanted IVC and SVC and their course to the mitral valve are difficult to assess. Cardiac 4D flow MRI readily depicts these features and provides information on blood flow variations in the Senning circulation (Fig 8).

Cardiac Valvular Disease

Cardiac 4D flow MRI allows accurate quantification of net flow volumes through all four cardiac valves (28). The regurgitation fraction can be assessed with good intra- and interobserver agreement (28).

Pulmonary and Aortic Regurgitation.—Two-dimensional cine PC sequences are widely used for MRI assessment of pulmonary regurgitation (29). Cardiac 4D flow MRI has shown good reliability and reproducibility for this indication (30) (Fig 9) (Movie 4). Cardiac 4D flow MRI helps achieve optimal positioning for blood flow measurements, avoiding the areas of vortical flow that may occur in an aneurysmal pulmonary artery (Fig 3c).

Similarly, reported measurement errors with 2D PC MRI can be avoided when estimating the regurgitation fraction and volume in patients with moderate to severe aortic regurgitation and sinus of Valsalva dilatation (31). In patients with significant aortic regurgitation, major vortical diastolic reverse flow imposes an eccentric systolic course on the systolic outflow jet along the outer wall of the ascending aorta (Figs 10, 11) (Movie

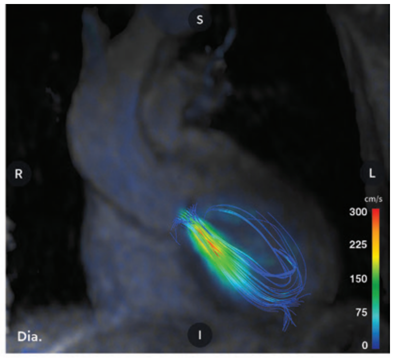

a.

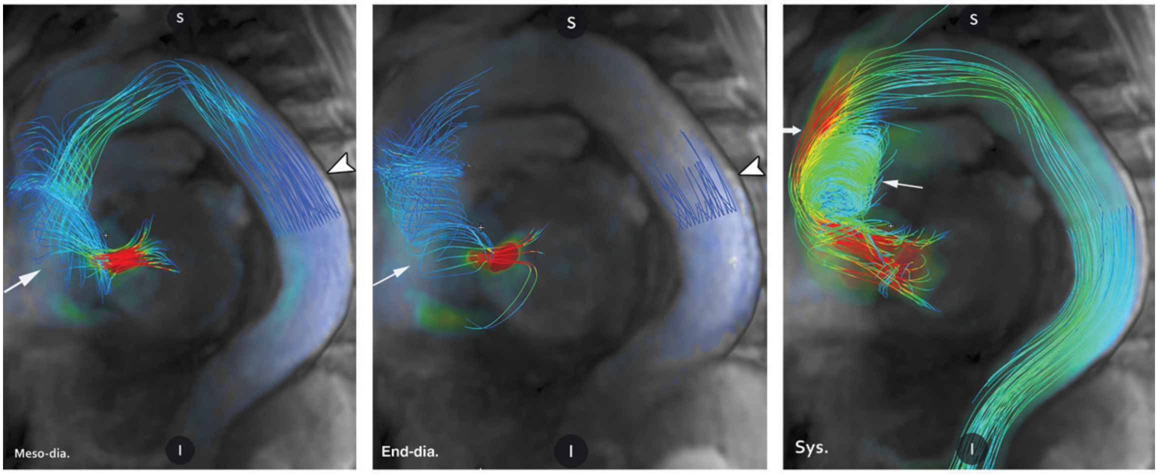

b. c. d.

Figure 10. Moderate aortic regurgitation visualized with cardiac 4D flow MRI in a middle-aged patient without significant aortic dilatation. **(a)** Image from diastole *(Dia)* shows aortic regurgitation assessed just above the aortic valve to avoid other aortic turbulent flows. **(b)** Image with streamlines from early diastole *(dia)* shows significant reverse flow in the descending aorta (arrowhead) and vortical flow starting in the ascending aorta (arrow). **(c)** Vortical flow in the ascending aorta (arrow) increases during diastole *(dia)*, while reverse flow in the descending aorta (arrowhead) decreases. **(d)** Image with streamlines from early systole *(Sys)* shows persistent vortical reverse flow (thin arrow) imposing an eccentric course to the systolic outflow jet along the outer wall of the ascending aorta (thick arrow).

5). Further large studies are needed to test the accuracy of cardiac 4D flow MRI in enabling discrimination between moderate and severe aortic regurgitation.

Mitral and Tricuspid Regurgitation.—Regurgitation through the atrioventricular valves can be assessed using 4D velocity acquisition (Movie 6). Four-dimensional proximal isovelocity surface area measurement may contribute to quantitate mitral regurgitation without making any geometric assumptions (32). Echocardiography is the first-line imaging investigation for evaluating mitral regurgitation, but cardiac 4D flow MRI can help assess regurgitation severity in complex cases with eccentric mitral regurgitation (33) (Fig 12).

Aortic Stenosis.—Phantom and in vivo studies in patients with aortic stenosis showed promising results with cardiac 4D flow MRI, although further validation is required (34). Evaluation of turbulence kinetic energy using cardiac 4D flow MRI may provide complementary information to that of echocardiography for discriminating between moderate and severe aortic stenosis.

Prosthetic Valve.—Cardiac 4D flow MRI allows assessment of blood flow after bioprosthetic valve surgery or transcatheter aortic valve implantation (TAVI) with minimal susceptibility artifacts (Fig 13) (Movie 7). Flow patterns and turbulence intensity downstream from a prosthetic heart valve are dependent on the specific valve design (35). Improved understanding of the hemodynamic consequences of percutaneous or open interventions may contribute to optimize treatment strategies.

Dilated Cardiomyopathy.—Changes in the extent and size of rotating vortices, as well as other flow alterations such as a decrease in direct flows, have been reported (36) and deserve further investigation.

Abnormalities of the Great Vessels

Early in vivo studies of cardiac 4D flow MRI evaluated blood flow path lines in the thoracic aorta and 3D quantification of thoracic aorta hemodynamics (37,38). The comprehensive evaluation of great vessel blood flow features provided by cardiac 4D flow MRI was first used by researchers, then shown to provide clinically relevant findings (6,39).

Bicuspid Aortic Valve and Aortic Aneurysm.—
Patients with bicuspid aortic valve (BAV) are at

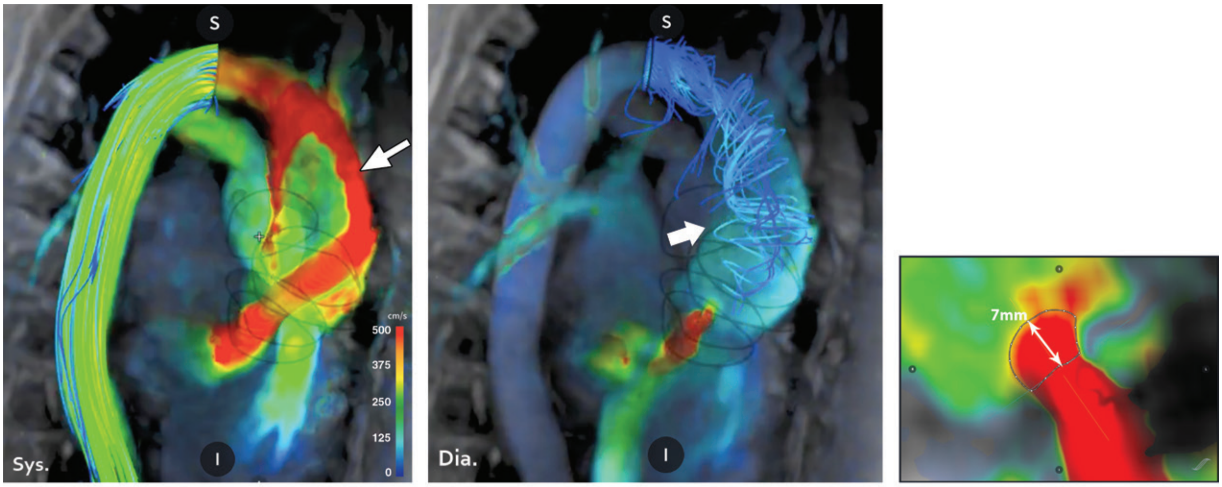

a. b. c.

Figure 11. Severe aortic regurgitation visualized with cardiac 4D flow MRI in a 68-year-old woman with aortic dilatation. **(a)** Three-dimensional velocity maximum intensity projection during systole *(Sys)* shows a high-velocity eccentric outflow jet along the outer wall of the aneurysmal ascending aorta (arrow). **(b)** Image with streamlines during diastole *(Dia)* shows marked vortical reverse flow starting from the aortic arch (arrow). **(c)** Routinely assessed echocardiographic parameters such as proximal isovelocity surface area measured by flow convergence and vena contracta width can also be measured using cardiac 4D flow MRI.

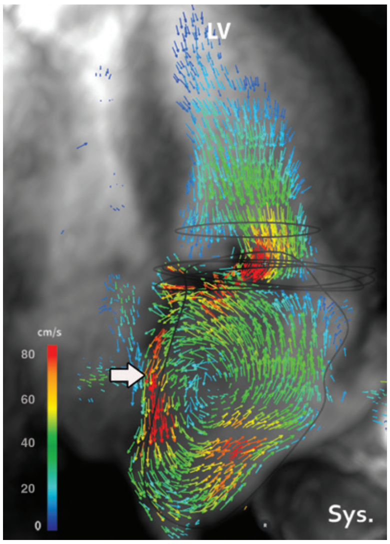

Figure 12. Severe complex mitral regurgitation in a 52-year-old woman. Cardiac 4D flow MRI was performed to better assess mitral regurgitation that was difficult to characterize with transthoracic echocardiography. Image with velocity vectors shows the course of a high-velocity eccentric jet (arrow). Note the marked vortical flows in the dilated left atrium during systole *(Sys)*. *LV* = left ventricle.

risk for ascending aortic aneurysm and dissection. Although vascular tissue changes have been described, BAV also induces hemodynamic flow turbulence that may contribute to aneurysm formation and growth (39). Recent data obtained using cardiac 4D flow MRI include high-velocity eccentric flow jets associated with changes in regional WSS distribution related to the aortic alterations seen in BAV. Flow eccentricity was the feature that was most sensitive to differences in BAV phenotype. WSS or jet impingement angle and jet flow eccentricity measured with cardiac 4D flow MRI may improve risk stratification in patients with ascending aortic aneurysms.

Vortices in the sinuses of Valsalva have been studied after different valve-sparing aortic root replacement procedures. The results contribute to the ongoing debate about the role of the sinuses and the importance of preserving them in valve-sparing surgical repair of aortic root ectasia (7,8,39). In patients with BAV, the WSS increase in the ascending aorta was most pronounced in the presence of aortic stenosis and in the absence of dilatation of the ascending aorta (40).

Aortic Coarctation.—Cardiac 4D flow MRI has been found reliable for assessing aortic coarctation and evaluating collateral blood flow in untreated patients and after repair surgery (40–42) (Fig 14) (Movie 8). Various methods of estimating pressure difference maps derived from cardiac 4D flow MRI have been described for depicting alterations in spatial pressure distribution in patients with repaired and unrepaired aortic coarctation (19,43). Further validation of these methods is needed.

Takayasu Disease.—Four-dimensional flow MRI may supply clinically relevant information in patients with inflammatory or noninflammatory aortic disease. Coronal acquisition and enhanced 4D flow MRI enable extensive coverage in an acquisition time of 8–10 minutes. Thus, the aorta can be covered from the proximal cerebral arteries to the aortic bifurcation (Fig

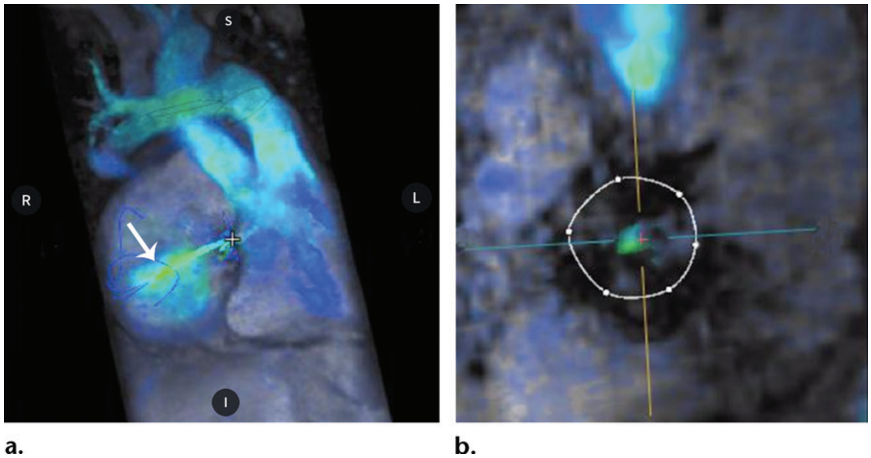

Figure 13. Cardiac 4D flow MRI after tricuspid bioprosthetic valve replacement. **(a)** Image with streamlines shows systolic central regurgitation (arrow). Artifacts are negligible, allowing assessment of tricuspid regurgitation flow, which may be difficult to achieve with echocardiography. **(b)** Regurgitant fraction can be assessed at the tricuspid valve level or estimated by comparing pulmonary outflow to right ventricular stroke volume.

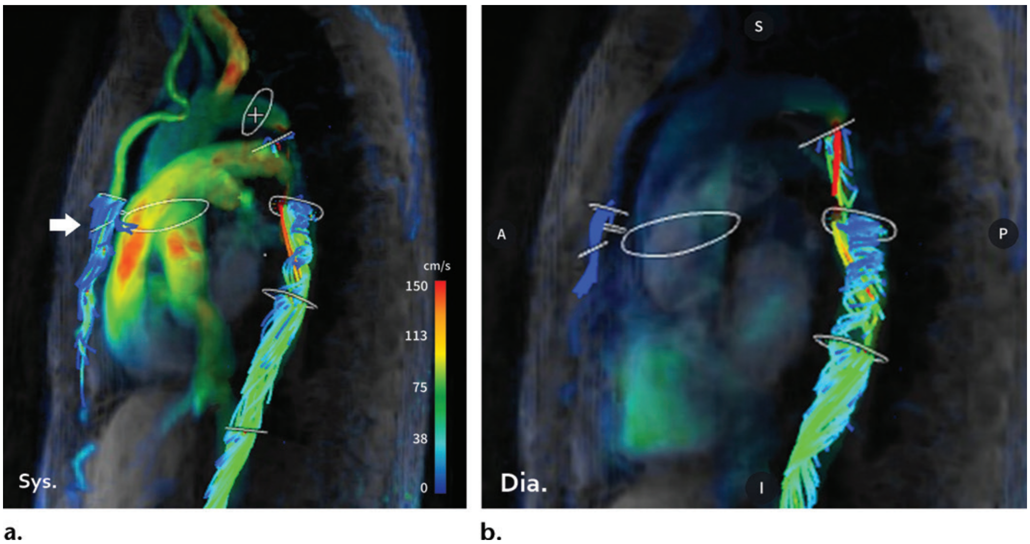

Figure 14. Cardiac 4D flow MRI of aortic coarctation in a 38-year-old man with systemic hypertension. Images with streamlines during systole *(Sys)* **(a)** and diastole *(Dia)* **(b)** show continuous systolic-diastolic low flow with a helical pattern downstream of the coarctation. Collateral flow through the large internal mammary arteries (arrow in **a**) was assessed and found to equal 35% of the flow through the descending aorta.

15). Blood flow data and regional WSS increases can be matched to anatomic changes such as wall thickening or aortic dilatation, ulceration, or stenosis (Fig 4).

Follow-up after Intervention.—Four-dimensional flow MRI at 1.5 T or 3 T can be used for follow-up after endovascular abdominal aortic aneurysm repair. Minimal artifacts are seen with these sequences, chiefly with the new nitinol endoprostheses. Four-dimensional flow MRI was more sensitive than CT angiography for detecting endoleaks (44). More interestingly, 4D flow MRI allows identification of concomitant multiple endoleaks, enables flow measurements, and shows via flow vector direction whether multiple vessels are involved in a type II endoleak (Fig 16).

Thus, 4D flow MRI allows subclassification of type II endoleaks into type IIa (biphasic flow pattern from a branch vessel) and type IIb (monophasic flow pattern with inflow and outflow branches) (44) (Movie 9), thereby improving interventional mapping for further embolization. Similarly, 4D flow MRI can provide useful information for follow-up of type B dissection after endovascular thoracic aorta repair (Fig 17) (Movie 10).

Pulmonary Hypertension.—Alterations in pulmonary artery flow hemodynamics have been

RadioGraphics

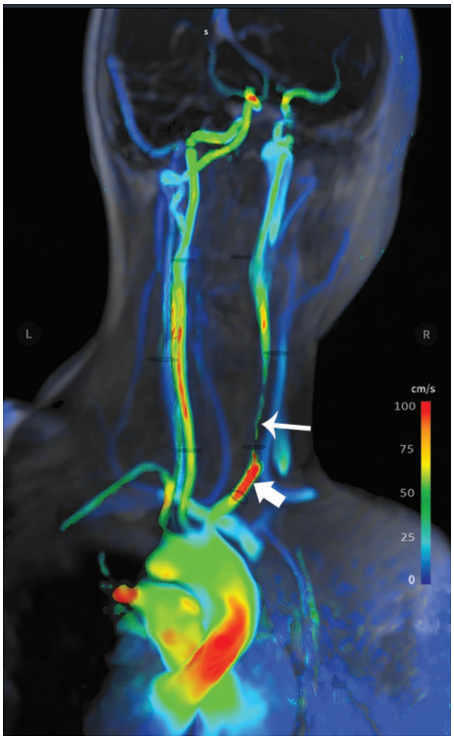

Figure 15. Four-dimensional flow MRI covering the thoracic aorta and cerebral arteries. Three-dimensional velocity rendering shows increased velocity in the proximal right common carotid artery (thick arrow) upstream of a long segment of tight stenosis (thin arrow). Note that the right subclavian artery is occluded.

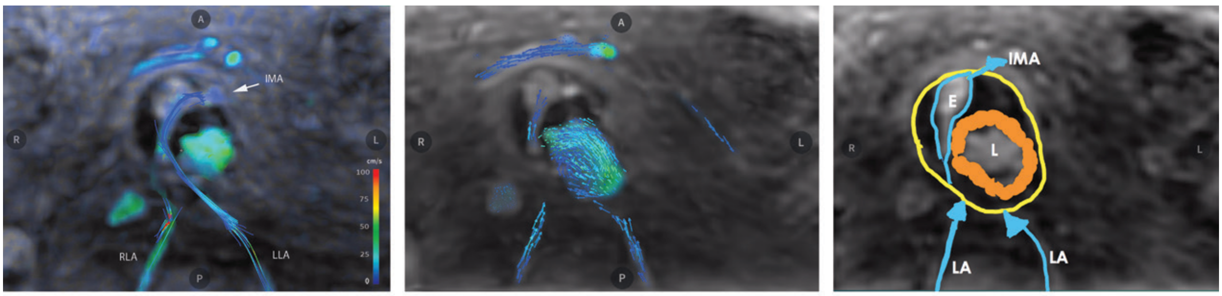

a. b. c.

Figure 16. Four-dimensional flow MRI after endovascular abdominal aortic aneurysm repair. **(a)** Image with streamlines shows that both L3 lumbar arteries and the inferior mesenteric artery *(IMA)* are involved in a type II endoleak. **(b, c)** Image with velocity vectors **(b)** allows subclassification of the endoleak as type IIb, with two inflow branches (both lumbar arteries) and one outflow branch (IMA) **(c)**. *E* = endoleak, *L* = aortic lumen, *LA* = lumbar artery.

abundantly documented in patients with pulmonary hypertension. Diastolic vorticity has been described as an indicator of mild pulmonary hypertension, whereas vorticity that becomes systolic indicates severe pulmonary hypertension (45). Helicity has also been found to have strong diagnostic potential, suggesting that characterizing flow hemodynamics may become an important component of the initial and follow-up evaluations in patients with pulmonary hypertension (45).

Increasing Number of New Applications

The field of application is expanding steadily. Thus, 4D flow MRI has been studied in portal hypertension (46), cerebral aneurysm risk stratification (47), and complex arteriovenous malformations (48) (Fig 18). The development of new sequences and technological advances can be expected to shorten acquisition times (49) and make postprocessing easier and faster, thus facilitating use of 4D flow MRI in clinical practice and allowing broader investigations in larger patient cohorts to further validate the technique in various applications.

When to Choose between 2D PC and 4D Flow MRI?

Through-plane 2D PC sequences are used in clinical routine, during breath holding, mostly for quantifying aortic or pulmonary artery blood flow. When the anatomic morphology of the patient is not complex and the patient can achieve breath holds, 2D PC MRI is a suitable

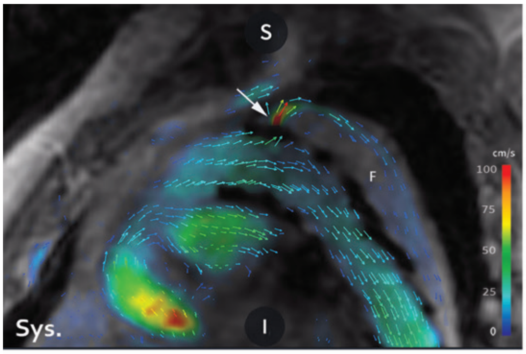

a.

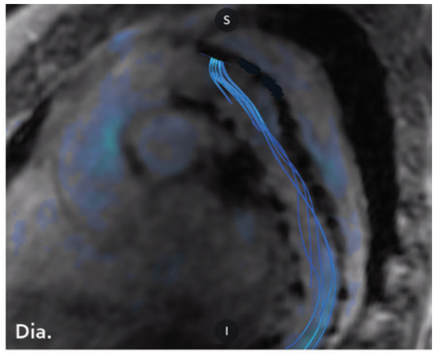

b.

Figure 17. Type I endoleak shown by 4D flow MRI in a patient with a thoracic stent-graft after type B aortic dissection. **(a)** Image with velocity vectors shows the inflow course of the type I endoleak (arrow) within the false lumen *(F)*. *Sys* = systole. **(b)** Image with streamlines shows outflow back to the aortic lumen during diastole *(Dia)* owing to higher pressure in the false lumen.

and fast method to assess valvular regurgitation or left-to-right shunting using the pulmonary-to-systemic blood flow ratio (Q_P/Q_S).

When placement of the acquisition plane is challenging, the number of measurements is elevated, anatomic features of the disease are complex (as in CHD), and breath holding is difficult, 4D flow MRI will be more accurate. Turbulent aortic flows due to a bicuspid aortic valve or aneurysmal ascending aorta will also be more accurately assessed with 4D flow sequences, with retrospective placement of the measurement plane avoiding the helical or vortical flow areas. Differences between 2D PC and 4D flow measurements were found—especially for the widely used ascending aorta flow—by Bollache et al (50), indicating that reference values should be established for each technique.

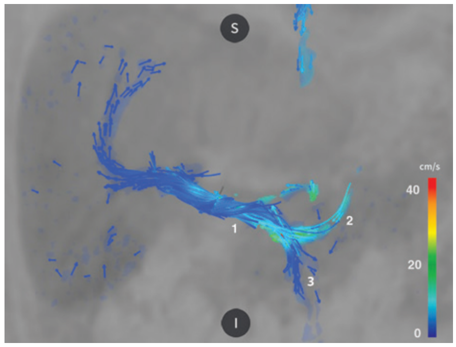

Figure 18. Suspected congestive hepatopathy in a 30-year-old woman years after Fontan operation. Image from 4D flow MRI shows normal and continuous flow in the portal vein *(1)*, with laminar helical flow seen after the confluence of the splenic vein *(2)* and superior mesenteric vein *(3)*. Velocity vectors demonstrate normal continuous hepatopetal flow.

Conclusion

Recent advances in 4D flow MRI have expanded the potential for assessing cardiovascular disease, thereby providing unprecedented capabilities for comprehensive quantitative evaluation of cardiovascular blood flows. Technological advances are now taking these capabilities into the realm of clinical practice. Early studies suggest that 4D flow MRI can play an important complementary role in cardiovascular assessments. New areas of application are emerging at a brisk pace. Multicenter studies in larger patient cohorts are needed for further validation. Four-dimensional flow MRI may soon become the reference standard for blood flow assessment in many indications.

Acknowledgments.—We would like to thank Arterys for their help in the preparation of the figures. We would also like to thank our technologist team and in particular Arnaud Fournier, Isaures de Chabannes, and Caroline Pasquet for their help in the elaboration of 4D flow sequences.

***Disclosures of Conflicts of Interest.*—A.A.** *Activities related to the present article:* consultant for Arterys. *Activities not related to the present article:* development of educational presentations for Guerbet. *Other activities:* disclosed no relevant relationships.

References

1. Bryant DJ, Payne JA, Firmin DN, Longmore DB. Measurement of flow with NMR imaging using a gradient pulse and phase difference technique. J Comput Assist Tomogr 1984;8(4):588–593.
2. Pelc NJ, Herfkens RJ, Shimakawa A, Enzmann DR. Phase contrast cine magnetic resonance imaging. Magn Reson Q 1991;7(4):229–254.
3. Srichai MB, Lim RP, Wong S, Lee VS. Cardiovascular applications of phase-contrast MRI. AJR Am J Roentgenol 2009;192(3):662–675.
4. Kilner PJ, Yang GZ, Mohiaddin RH, Firmin DN, Longmore DB. Helical and retrograde secondary flow patterns in the aortic arch studied by three-directional magnetic resonance velocity mapping. Circulation 1993;88(5 Pt 1):2235–2247.
5. Markl M, Chan FP, Alley MT, et al. Time-resolved three-dimensional phase-contrast MRI. J Magn Reson Imaging 2003;17(4):499–506.
6. Markl M, Kilner PJ, Ebbers T. Comprehensive 4D velocity mapping of the heart and great vessels by cardiovascular magnetic resonance. J Cardiovasc Magn Reson 2011;13(1):7.
7. Dyverfeldt P, Bissell M, Barker AJ, et al. 4D flow cardiovascular magnetic resonance consensus statement. J Cardiovasc Magn Reson 2015;17(1):72.

8. Uribe S, Beerbaum P, Sørensen TS, Rasmusson A, Razavi R, Schaeffter T. Four-dimensional (4D) flow of the whole heart and great vessels using real-time respiratory self-gating. Magn Reson Med 2009;62(4):984–992.
9. Dyverfeldt P, Ebbers T. Comparison of respiratory motion suppression techniques for 4D flow MRI. Magn Reson Med 2017;78(5):1877–1882.
10. Bock J, Frydrychowicz A, Stalder AF, et al. 4D phase contrast MRI at 3 T: effect of standard and blood-pool contrast agents on SNR, PC-MRA, and blood flow visualization. Magn Reson Med 2010;63(2):330–338.
11. Hadizadeh DR, Jost G, Pietsch H, et al. Intraindividual quantitative and qualitative comparison of gadopentetate dimeglumine and gadobutrol in time-resolved contrast-enhanced 4-dimensional magnetic resonance angiography in minipigs. Invest Radiol 2014;49(7):457–464.
12. Schnell S, Ansari SA, Wu C, et al. Accelerated dual-venc 4D flow MRI for neurovascular applications. J Magn Reson Imaging 2017;46(1):102–114.
13. Buonocore MH. Visualizing blood flow patterns using streamlines, arrows, and particle paths. Magn Reson Med 1998;40(2):210–226.
14. Markl M, Wallis W, Harloff A. Reproducibility of flow and wall shear stress analysis using flow-sensitive four-dimensional MRI. J Magn Reson Imaging 2011;33(4):988–994.
15. Bürk J, Blanke P, Stankovic Z, et al. Evaluation of 3D blood flow patterns and wall shear stress in the normal and dilated thoracic aorta using flow-sensitive 4D CMR. J Cardiovasc Magn Reson 2012;14(1):84.
16. Doddasomayajula R, Chung BJ, Mut F, et al. Hemodynamic characteristics of ruptured and unruptured multiple aneurysms at mirror and ipsilateral locations. AJNR Am J Neuroradiol 2017;38(12):2301–2307.
17. Bolster BD Jr, Atalar E, Hardy CJ, McVeigh ER. Accuracy of arterial pulse-wave velocity measurement using MR. J Magn Reson Imaging 1998;8(4):878–888.
18. Yang GZ, Kilner PJ, Wood NB, Underwood SR, Firmin DN. Computation of flow pressure fields from magnetic resonance velocity mapping. Magn Reson Med 1996;36(4):520–526.
19. Rengier F, Delles M, Eichhorn J, et al. Noninvasive pressure difference mapping derived from 4D flow MRI in patients with unrepaired and repaired aortic coarctation. Cardiovasc Diagn Ther 2014;4(2):97–103.
20. Maceira AM, Prasad SK, Khan M, Pennell DJ. Reference right ventricular systolic and diastolic function normalized to age, gender and body surface area from steady-state free precession cardiovascular magnetic resonance. Eur Heart J 2006;27(23):2879–2888.
21. Kilner PJ, Gatehouse PD, Firmin DN. Flow measurement by magnetic resonance: a unique asset worth optimising. J Cardiovasc Magn Reson 2007;9(4):723–728.
22. Devos DG, Kilner PJ. Calculations of cardiovascular shunts and regurgitation using magnetic resonance ventricular volume and aortic and pulmonary flow measurements. Eur Radiol 2010;20(2):410–421.
23. Valente AM, Sena L, Powell AJ, Del Nido PJ, Geva T. Cardiac magnetic resonance imaging evaluation of sinus venosus defects: comparison to surgical findings. Pediatr Cardiol 2007;28(1):51–56.
24. Kilner PJ. Imaging congenital heart disease in adults. Br J Radiol 2011;84(Spec No 3):S258–S268.
25. Valverde I, Nordmeyer S, Uribe S, et al. Systemic-to-pulmonary collateral flow in patients with palliated univentricular heart physiology: measurement using cardiovascular magnetic resonance 4D velocity acquisition. J Cardiovasc Magn Reson 2012;14(1):25.
26. Sjöberg P, Heiberg E, Wingren P, et al. Decreased diastolic ventricular kinetic energy in young patients with Fontan circulation demonstrated by four-dimensional cardiac magnetic resonance imaging. Pediatr Cardiol 2017;38(4):669–680 [published correction appears in Pediatr Cardiol 2017;38(5):1087].
27. Geiger J, Markl M, Jung B, et al. 4D-MR flow analysis in patients after repair for tetralogy of Fallot. Eur Radiol 2011;21(8):1651–1657.
28. Westenberg JJ, Roes SD, Ajmone Marsan N, et al. Mitral valve and tricuspid valve blood flow: accurate quantification with 3D velocity-encoded MR imaging with retrospective valve tracking. Radiology 2008;249(3):792–800.
29. Davlouros PA, Kilner PJ, Hornung TS, et al. Right ventricular function in adults with repaired tetralogy of Fallot assessed with cardiovascular magnetic resonance imaging: detrimental role of right ventricular outflow aneurysms or akinesia and adverse right-to-left ventricular interaction. J Am Coll Cardiol 2002;40(11):2044–2052.
30. Chelu RG, Wanambiro KW, Hsiao A, et al. Cloud-processed 4D CMR flow imaging for pulmonary flow quantification. Eur J Radiol 2016;85(10):1849–1856.
31. Muzzarelli S, Monney P, O'Brien K, et al. Quantification of aortic flow by phase-contrast magnetic resonance in patients with bicuspid aortic valve. Eur Heart J Cardiovasc Imaging 2014;15(1):77–84.
32. Gorodisky L, Agmon Y, Porat M, Abadi S, Lessick J. Assessment of mitral regurgitation by 3-dimensional proximal flow convergence using magnetic resonance imaging: comparison with echo-Doppler. Int J Cardiovasc Imaging 2018;34(5):793–802.
33. Nordmeyer S, Riesenkampff E, Messroghli D, et al. Four-dimensional velocity-encoded magnetic resonance imaging improves blood flow quantification in patients with complex accelerated flow. J Magn Reson Imaging 2013;37(1):208–216.
34. Binter C, Gotschy A, Sündermann SH, et al. Turbulent kinetic energy assessed by multipoint 4-dimensional flow magnetic resonance imaging provides additional information relative to echocardiography for the determination of aortic stenosis severity. Circ Cardiovasc Imaging 2017;10(6):e005486.
35. Kvitting JP, Dyverfeldt P, Sigfridsson A, et al. In vitro assessment of flow patterns and turbulence intensity in prosthetic heart valves using generalized phase-contrast MRI. J Magn Reson Imaging 2010;31(5):1075–1080.
36. Carlhäll CJ, Bolger A. Passing strange: flow in the failing ventricle. Circ Heart Fail 2010;3(2):326–331.
37. Bogren HG, Buonocore MH. 4D magnetic resonance velocity mapping of blood flow patterns in the aorta in young vs. elderly normal subjects. J Magn Reson Imaging 1999;10(5):861–869.
38. Bogren HG, Buonocore MH, Valente RJ. Four-dimensional magnetic resonance velocity mapping of blood flow patterns in the aorta in patients with atherosclerotic coronary artery disease compared to age-matched normal subjects. J Magn Reson Imaging 2004;19(4):417–427.
39. Mahadevia R, Barker AJ, Schnell S, et al. Bicuspid aortic cusp fusion morphology alters aortic three-dimensional outflow patterns, wall shear stress, and expression of aortopathy. Circulation 2014;129(6):673–682.
40. Farag ES, van Ooij P, Planken RN, et al. Aortic valve stenosis and aortic diameters determine the extent of increased wall shear stress in bicuspid aortic valve disease. J Magn Reson Imaging 2018;48(2):522–530.
41. Hope MD, Meadows AK, Hope TA, et al. Clinical evaluation of aortic coarctation with 4D flow MR imaging. J Magn Reson Imaging 2010;31(3):711–718.
42. Charpentier E, Bacquet D, Pontnau F, Azarine A. Asymptomatic aortic coarctation diagnosed because of large abdominal arterial collateral. Vasc Med 2017;22(4):347–348.
43. Bock J, Frydrychowicz A, Lorenz R, et al. In vivo noninvasive 4D pressure difference mapping in the human aorta: phantom comparison and application in healthy volunteers and patients. Magn Reson Med 2011;66(4):1079–1088.
44. Sakata M, Takehara Y, Katahashi K, et al. Hemodynamic analysis of endoleaks after endovascular abdominal aortic aneurysm repair by using 4-dimensional flow-sensitive magnetic resonance imaging. Circ J 2016;80(8):1715–1725.
45. Reiter G, Reiter U, Kovacs G, Olschewski H, Fuchsjäger M. Blood flow vortices along the main pulmonary artery measured with MR imaging for diagnosis of pulmonary hypertension. Radiology 2015;275(1):71–79.
46. Roldán-Alzate A, Frydrychowicz A, Niespodzany E, et al. In vivo validation of 4D flow MRI for assessing the hemodynamics of portal hypertension. J Magn Reson Imaging 2013;37(5):1100–1108.

47. Futami K, Nambu I, Kitabayashi T, et al. Inflow hemodynamics evaluated by using four-dimensional flow magnetic resonance imaging and the size ratio of unruptured cerebral aneurysms. Neuroradiology 2017;59(4):411–418.
48. Legras A, Azarine A, Poitier B, Messas E, Le Pimpec-Barthes F. Systemic artery to pulmonary vein fistula after right upper lobectomy demonstrated by 4-dimensional flow magnetic resonance imaging. Ann Thorac Surg 2017;104(2):e169–e171.
49. Dyvorne H, Knight-Greenfield A, Jajamovich G, et al. Abdominal 4D flow MR imaging in a breath hold: combination of spiral sampling and dynamic compressed sensing for highly accelerated acquisition. Radiology 2015;275(1):245–254.
50. Bollache E, van Ooij P, Powell A, Carr J, Markl M, Barker AJ. Comparison of 4D flow and 2D velocity-encoded phase contrast MRI sequences for the evaluation of aortic hemodynamics. Int J Cardiovasc Imaging 2016;32(10):1529–1541.

This journal-based SA-CME activity has been approved for ***AMA PRA Category 1 Credit™.*** *See rsna.org/learning-center-rg.*